Journal of Marine Science and Technology

Volume 27 | Issue 2 Article 5

# EQUIVALENT NUMERICAL ALGORITHM FOR THE STRIP-ROLLING PROCESS OF A CONTINUOUS VARIABLE CROWN MILL USING THE COUPLED RIGID-PLASTIC FINITE ELEMENT METHOD

Tao Wang
*College of Mechanical and Vehicle Engineering, Taiyuan University of Technology, Taiyuan, China.*

Zhong-Kai Ren
*College of Mechanical and Vehicle Engineering, Taiyuan University of Technology, Taiyuan, China.*,
zhongkai_0808@126.com

Dong-Ping He
*College of Mechanical and Vehicle Engineering, Taiyuan University of Technology, Taiyuan, China.*



## Recommended Citation

Wang, Tao; Ren, Zhong-Kai; and He, Dong-Ping (2019) "EQUIVALENT NUMERICAL ALGORITHM FOR THE STRIP-ROLLING PROCESS OF A CONTINUOUS VARIABLE CROWN MILL USING THE COUPLED RIGID-PLASTIC FINITE ELEMENT METHOD," *Journal of Marine Science and Technology*: Vol. 27: Iss. 2, Article 5.
DOI: 10.6119/JMST.201904_27(2).0005
Available at: https://jmstt.ntou.edu.tw/journal/vol27/iss2/5

# EQUIVALENT NUMERICAL ALGORITHM FOR THE STRIP-ROLLING PROCESS OF A CONTINUOUS VARIABLE CROWN MILL USING THE COUPLED RIGID-PLASTIC FINITE ELEMENT METHOD

## Acknowledgements

This project are supported by Major program of national natural science foundation of China (Grant No. U1710254), National natural science foundation of China (Grant No. 51804215), Shanxi Province science and technology major project (Grant No. MC2016-01), Shanxi province science and technology major projects (Grant No. 20181102015), Natural science foundation of Shanxi Province (Grant No. 201701D221143), Taiyuan city science and technology major projects (Grant No. 170203), key research and development program of Shanxi Province (Grant No. 201703D111003). R

*Journal of Marine Science and Technology, Vol. 27, No. 2, pp. 123-132 (2019)*
DOI: 10.6119/JMST.201904_27(2).0005


# EQUIVALENT NUMERICAL ALGORITHM FOR THE STRIP-ROLLING PROCESS OF A CONTINUOUS VARIABLE CROWN MILL USING THE COUPLED RIGID-PLASTIC FINITE ELEMENT METHOD

Tao Wang, Zhong-Kai Ren, and Dong-Ping He

Key words: continuous variable crown, rigid-plastic finite element method, equivalent algorithm, efficiency.

## ABSTRACT

For the accurate simulation of the rolling process of a wide strip and plates, highly sophisticated algorithms must be developed to couple material flow behavior with the elastic deformation of rolls. A coupling simulation system based on a three-dimensional rigid-plastic finite element method (RPFEM), elastic-plastic finite element method, and influential function method was developed in this study. Calculation of the continuous variable crown (CVC) mill was more complex than that of the normal 4-high rolling mill. According to the point symmetry of the roll gap profile, the CVC curves of work rolls at various shifting positions were equal to various work roll crowns in normal 4-high mills. Thus, an equivalent model that adopts a 1/4 workpiece for calculation using the RPFEM can be employed to analyze metal deformation. Based on the approximate symmetrical distribution of rolling force, the influential function method was applied to solve the overall elastic deformation of all upper rolls. Thus, reliable results concerning profile transfer and tension distribution were obtained by the coupling the strip model alongside routines for elastic roll stack deflection. The results revealed that the equivalent algorithm can reduce the number of iterations by approximately 50% and the computation time by approximately 80% compared with the traditional algorithm.

## I. INTRODUCTION

Continuous variable crown (CVC) technology was developed by the SMS Company in the late 1970s to control the crown and flatness of strips (Kawanami et al., 1983; Wood et al., 1989). The fundamental principle is that the profile of the two rolls is ground into a shape that is similar to the "~" symbol in appearance, and the rolls have opposing configurations. An antisymmetrical roll gap between the two rolls can be formed because of the special roll shape. Thickness variation in the rolled sheet between the roll gaps in the width direction can be achieved by shifting the two work rolls in the opposite axial directions.

To achieve high-quality control of the rolling process, high-precision CVC rolling process simulation models are required to manufacture high-quality products that meet even the strictest tolerance requirements. Linghu (Linghu et al., 2014) developed a three-dimensional (3D) elastic-plastic finite element (FE) model of cold strip rolling for a 6-high CVC control rolling mill. The boundary conditions, including accurate CVC curves, total rolling force, total bending force, and roll shifting value, were considered in this model. Kim (Kim et al., 2003) presented an integrated FE process model for the coupled analysis of mechanical strip behavior. That model may reflect the detailed aspects of various process variables in the strip profile. Wang (Wang et al.,2005) used the stream surface element method and influential function method to analyze 3D plastic deformation of the strip and elastic deformation of rolls, respectively. Continuous hot rolling processes were employed to simulate the factor of strip width in this method. Using ANSYS, an analysis of a roll backup contact deformation system for a 6-high CVC cold rolling mill was conducted by Zhang (Zhang et al., 2007). Daun (Daun et al., 2013) proposed a 3D simulator for the rough rolling process using the FE method (FEM) to effectively reduce camber and side slipping and achieve a reasonable wedge profile. Du (Wang et al., 2005; Du et al., 2007) conducted a simulation of the cross wedge rolling process using the FE software program DEFROM-3D alongside coupled thermomechanical and microstructural evolution. Kainz (Kainz, 2013) proposed an enhanced iterative algorithm for the effective numerical simulation of the contact between an elastic roll stack and an elastoviscoplastic strip or plate in hot rolling.

As shown in related studies, 3D FE models can predict not only actual metal deformation fields but also accurate strip crown and flatness results (Hwang et al., 2002; Kim et al., 2005; Wang

*Paper submitted 04/20/18; revised 08/22/18; accepted 03/05/19. Author for correspondence: Zhong-Kai Ren (e-mail: zhongkai_0808@126.com).*
*College of Mechanical and Vehicle Engineering, Taiyuan University of Technology, Taiyuan, China.*

et al., 2012; Nakhoul et al., 2014; Lee et al., 2016). However, the simulation process is time consuming, regardless of whether commercial software or computer programs developed by researchers are used. To improve the efficiency of the rigid-plastic FEM (RPFEM), Wang (Liu and Wang, 2003) proposed a two-dimensional forecasting model to provide rolling force distribution as an initial iteration value of the 3D FEM and simulate the metal deformation process. Liu (Liu et al., 2004; Wang et al., 2012) presented a novel method termed the strip layer method to simulate the 3D deformation of the plate and strip-rolling process. Chen (Chen et al., 2012; Wang et al., 2015) presented a numerical analysis of 3D rolling processing that combined the fast multiple method and boundary element method. Schmidtchen (Schmidtchen et al., 2016) developed a fast numerical simulation model for symmetrical flat-rolling processes based on an extended slab theory. For a CVC mill and pair cross mill, time consumption is at least doubled compared with a standard 4-high mill because of the meshing way of strip and rolls. Yanagimoto (Yanagimoto, 2002) proposed an equivalent model for a pair cross mill to reduce the number of elements in the 3D RPFEM. Therefore, a new coupled equivalent algorithm for a CVC mill based on the RPFEM for greater computation efficiency is proposed in this paper.

## II. COUPLING MODEL BASED ON THE RPFEM

### 1. Rigid-Plastic FE Formulation

The RPFEM based on a Lagrange multiplier was used to analyze the plastic deformation of workpieces in roll gap (Takaaki et al., 1991). The RPFEM can be inferred from the variation principle of rigid-plastic material. The energy consumption rate function is expressed as a nonlinear function of nodal velocities. According to optimization theory, a cinematically admissible velocity field can be obtained by minimizing the total energy consumption rate; deformation and mechanical parameters can then be solved.

The energy consumption rate function can be expressed as follows:

$$\phi = \int_V \bar{\sigma}\dot{\bar{\varepsilon}}dV - \int_{S_f} F_i v_i dS + \int_V \lambda \dot{\varepsilon}_{ij}\delta_{ij}dV \qquad (1)$$

where $\bar{\sigma}$ is the equivalent stress, $\dot{\bar{\varepsilon}}$ is the equivalent strain rate, $F_i$ is the imposed traction vector at the force boundary $S_f$, $v_i$ is the velocity, $\lambda$ is the Lagrange multiplier, $\dot{\varepsilon}_{ij}$ is the strain rate tensor, and $\delta_{ij}$ is the Kronecker delta.

To solve the velocity field and Lagrange multiplier, the equation is annihilated using the partial derivative of the energy consumption rate function. A normal 8-node hexahedral solid element is used to discretize the solution domain. Nonlinear equations are formed for nodal velocity, and Newton-Raphson iteration is adopted to solve the velocity field.

### 2. Multiparameter Coupling Model

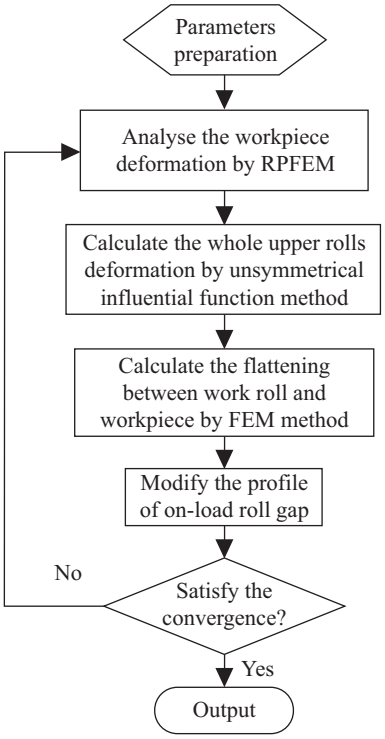


**Fig. 1. Flowchart of the coupling model for rolling process.**

The multi-parameter coupling model proposed in this paper involves the following interactive numerical procedures, the RPFEM for metal forming process, influential function method for roll bending deflection. The influential function method is a discretization method that originated from mathematical physics. The basic concept involves the division of the roll into several elements in the roll-body direction; the load and elastic deformation of the roll are discretized according to the same element. The elastic-plastic FEM (Liu et al., 1985) for flattening between a work roll and workpiece constitutes elastic deformation due to contact pressure, and the Foppl formula for flattening between a work roll and backup roll constitutes elastic deformation between two rolls due to contact pressure. Foppl theory assumes that a roll is semi-infinite, meaning that the length of the roll is infinite and the contact stress follows an elliptical distribution along the width of the contact zone. The requirements of rolling force balance and deformation compatibility between the interacting elastically deformed rolls and the plastically deformed workpiece can be satisfied by the coupling iterative numerical procedure shown in Fig. 1, as is the calculation flowchart for a normal 4-high mill.

The detailed iterative numerical procedure of the proposed coupling model is described as follows:

Step 1: Taking the roll gap profile after roll deflection calculation as the boundary condition (roll deflection is not considered in the first step), the RPFEM is used to analyze the workpiece in the roll gap, deformation, and the lateral distribution of rolling force.

Step 2: Taking the rolling force distribution as a boundary condition, the bending deformation of the rolls is calculated using the influential function method, and flattening between rolls is calculated using the Foppl formula. Then, taking the distribution of rolling force and elastic deformation of the roll as boundary conditions, flattening between the work rolls and workpiece is calculated using the 3D elastic-plastic FEM to obtain the gap distribution of the roll with load.

Step 3: The roll gap profile in step 1 is updated and the same process is repeated until the change in workpiece thickness is lower than the preset convergent value.

The transverse distribution of rolling pressure affects the shape of the roll gap, which in turn affects the transverse distribution of rolling pressure. Therefore, only by coupling the 3-D plastic deformation model with the roll system deformation model through the iterative scheme can the plate crown and shape be predicted accurately.

## III. EQUIVALENT CVC MILL MODEL

To improve the efficiency of the RPFEM coupling model, an equivalent model for the CVC mill ("ECVC model" hereafter) consisting of the 1/4 model to analyze metal plastic deformation and the 1/2 model to analyze roll elastic deformation is proposed in this paper.

To utilize the symmetrical feature, a quarter of the workpiece and rolls can be used to establish the FE mesh for a normal 4-high mill; only 10-20 minutes is required to simulate one rolling pass. By contrast, for the CVC mill with antisymmetrical features, a half model containing half a workpiece and all upper rolls is often used to construct the model, and simulating one rolling pass by using the same computer requires more than 3 hours. If an equivalent method can be found, the rolling process of the CVC mill can be considered a normal 4-high mill, and thus the simulation time can be greatly shortened.

In the rolling process of the CVC mill, the workpiece and roll system are antisymmetrical with respect to the center point. Compared with the original profile, the equivalent profile has identical thickness at any position along the workpiece width. Therefore, the half model of the workpiece in the CVC rolling process is simplified to the quarter model shown in Fig. 2, which can considerably simplify the calculation of the plastic deformation of the workpiece.

### 1. Equivalent Profile of the Roll Gap

The contour curve of the CVC work roll is similar in appearance to the "~" symbol. The upper and lower work rolls have a 180° antisymmetrical configuration. The equivalent roll crown of the quarter model, which replaces the roll crown of the original model, was analyzed. The coordinate system is shown in Fig. 3.

The roll radius function of the upper roll can be expressed as follows:

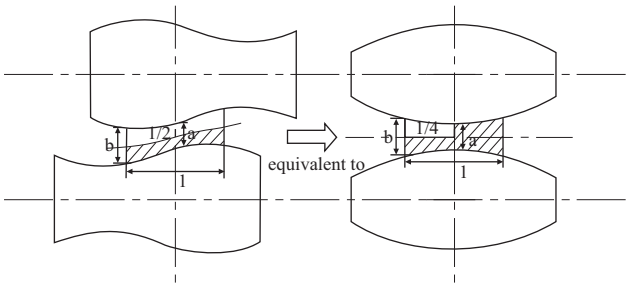


**Fig. 2. The diagram of traditional CVC model equivalent to the 1/4 model.**

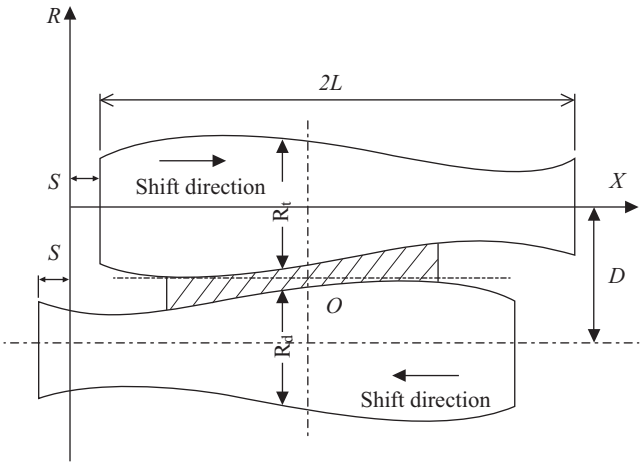


**Fig. 3. Schematic view of the CVC work roll profile.**

$$R_t(x) = A_0 + A_1 x + A_2 x^2 + A_3 x^3 \tag{2}$$

where $A_i\,(i = 1 \sim 3)$ is a constant of the work roll contour, and the specific reference is used in Table 1.

Because the lower roll has the same roll contour as the upper roll and is positioned antisymmetrically to the upper roll, the function of the lower roll radius can be expressed as follows:

$$R_d(x) = A_0 + A_1(2L - x) + A_2(2L - x)^2 + A_3(2L - x)^3 \tag{3}$$

where $L$ is one-half of the work roll length.

The upper roll radius after axial shifting can be expressed as follows:

$$R_t(x, s) = A_0 + A_1(x - s) + A_2(x - s)^2 + A_3(x - s)^3 \tag{4}$$

where $s$ is the distance of axis shifting.

The lower roll radius after axial shifting can be expressed as follows:

$$R_d(x, s) = A_0 + A_1(2L - x - s) + A_2(2L - x - s)^2 + A_3(2L - x - s)^3 \tag{5}$$

**Table 1. Parameters for CVC work roll profile.**

| $A_0$ | $A_1$ | $A_2$ | $A_3$ | 2L | $S_{max}$ |
|---|---|---|---|---|---|
| 424.975286 | 6.15108089E-4 | 1.02190713E-7 | -8.51583719E-10 | 2080 | ±150 |

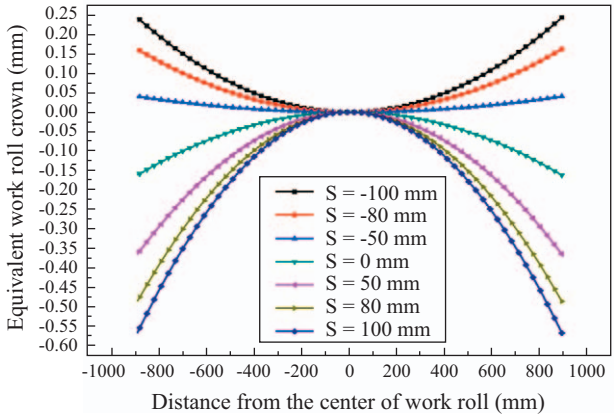


**Fig. 4. Relationship between equivalent work roll crown and shifting amount.**

The function of the roll gap profile after axis shifting can be expressed as follows:

$$\begin{aligned} g(x,s) &= D - R_t(x,s) - \mathrm{R_d}(x,s) \\ &= D - R_t(x,s) - R_t(2L-x,s) \end{aligned} \tag{6}$$

where $D$ is the distance between the upper and lower roll axes.

The equivalent crown of the work roll can be expressed as follows:

$$\begin{aligned} C_g &= g(L,s) - g(S_{\max},s) \\ &= -A_2\left[2(L-s)^2 - (S_{\max}-s)^2 - (2L-s-S_{\max})^2\right] \\ &\quad - A_3\left[2(L-s)^3 - (S_{\max}-s)^3 - (2L-s-S_{\max})^3\right] \end{aligned} \tag{7}$$

where $S_{max}$ is the maximum distance of axial shifting.

Fig. 4 shows the equivalent crown of the work roll at various shifting positions based on the parameters in Table 1.

## 2. Symmetrical Characteristic of Rolling Force Distribution

Rolling force distribution should be symmetrical because of the special work roll contour. If the axial shifting of the work rolls causes a significant difference in rolling force distribution between the left and right halves of the metal deformation zone, the quarter symmetrical model produces a significant error while attempting to solve the metal deformation problem. Therefore, an investigation of the asymmetric features of metal deformation and rolling force distribution between the work roll and deformed workpiece in the model is necessary.

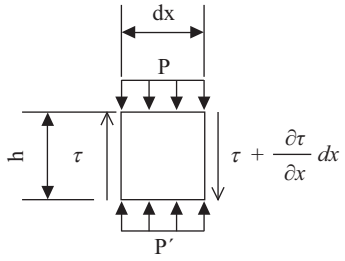


**Fig. 5. Micro element of a workpiece along with direction.**

Fig. 5 shows a microelement of a workpiece in the roll gap of the CVC mill. According to the force equilibrium relationship along the rolling gap, the following relationship is obtained:

$$p\,dx + \left(\tau + \frac{\partial \tau}{\partial x}dx\right)h = p'\,dx + \tau h \tag{8}$$

where $h$ is the thickness of the strip, $dx$ is the width of the microelement, $p$ is the uniform load on the upper surface of the strip, $p'$ is the uniform load on the lower surface of the strip, and $\tau$ is the shear stress.

This function can be simplified as follows:

$$p - p' = \frac{\partial \tau}{\partial x}h \tag{9}$$

where $\frac{\partial \tau}{\partial x}$ is the shear stress variation along the strip width. Because the ratio of width to thickness for the thin wide strip is extremely high, $\frac{\partial \tau}{\partial x}$ is low compared with the rolling force $p$, which is comparable to $p'$.

The parameters of the 2050 CVC hot rolling mill are shown in Table 2, and the rolling process parameters of the F1 stand and F3 stand are shown in Table 3. The rolling mill is treated as the research object, and the difference in rolling force between the left and right are calculated. The distribution of the difference along the width of the plate is shown in Fig. 6; the difference between the left and right rolling force does not exceed 20 N/mm, which is considerably lower than the order of magnitude of the rolling force. This result indicates that the symmetry of rolling force distribution is coordinated. Thus, the quarter rolling model can be used to calculate the distribution of rolling force and meet the accuracy requirement.

**Table 2. Basic parameters of 2050 CVC rolling mill.**

| Name | Value |
|---|---|
| F1-F3 work roll diameter (mm) | 807 |
| Length of work roll (mm) | 2250 |
| Original crown of work roll (mm) | 0 |
| Bending force of work roll (kN) | 500 |
| F1-F3 backup roll diameter (mm) | 1440 |
| Length of support roll (mm) | 2050 |
| Center distance of a hydraulic cylinder of the support roll (mm) | 3150 |
| Original crown of backup roll (mm) | 0 |
| strip width (mm) | 1350 |

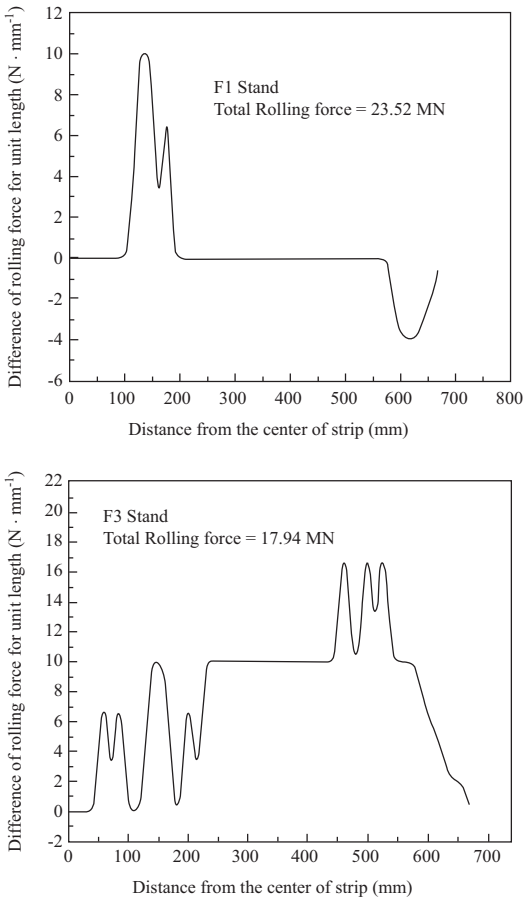


**Fig. 6. Difference of unit rolling force distribution.**

## 3. Establishment of the Equivalent Model

A combined arithmetic calculation is proposed to make full use of the efficiency of the quarter model and the accuracy of the results of the half model. The CVC curve and axial shifting are equal to the work roll crown of the normal 4-high mill. The quarter model of the workpiece and rolls can be used to calculate the rolling force by using the RPFEM. Based on the aforementioned theory, the rolling force distribution is almost symmetrical. The half model (i.e., all upper rolls that have the CVC curve) can be employed to analyze roll deflection. The equivalent model meets not only the requirement of having unsymmetrical work roll contours but also those of high efficiency and accuracy.

**Table 3. The rolling process parameters of F1 and F3 stand.**

| Stand | F1 | F3 |
|---|---|---|
| Inlet thickness (mm) | 46.19 | 19.28 |
| Exit thickness (mm) | 29.64 | 13.76 |
| Front tension (MPa) | 3.79 | 5.59 |
| Rolling temperature (°C) | 957 | 929 |
| Bending force (kN) | 952 | 951 |
| Shifting displacement (mm) | 90 | 90 |

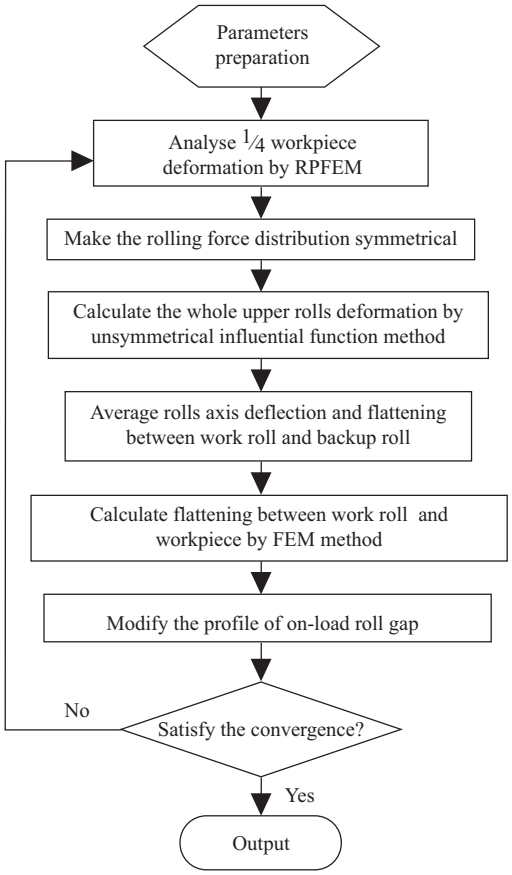


**Fig. 7. Calculating flowchart for ECVC model.**

The half model for roll deformation can predict the unsymmetrical distributions of rolling force between the work roll and backup roll, as well as the axis deflection and the flattening of all upper rolls. Only half of the on-load roll gap profile is required for the quarter model. An average procedure was proposed to deal with the coupling relationship between the quarter model and half model. Although the roll axis deflection and flattening of the two models differed, the crown of the on-load roll gaps and the rolling force distribution were comparable. The flowchart for the ECVC model is shown in Fig. 7.

**Table 4. Calculating parameters.**

| Rolling width (mm) | Inlet/exit thickness (mm) | Rolling temperature (°C) | Rolling speed (mm/s) | Tension (MPa) | Bending force (t/chock) | Friction coefficient | Flow stress (MPa) | Material |
|---|---|---|---|---|---|---|---|---|
| 1100 | 14.4/9.5 | 923.8 | 4036 | 7.8/5.1 | 0 | 0.29 | $175\bar{\varepsilon}^{0.21}\dot{\bar{\varepsilon}}^{0.13}$ | Q235 |

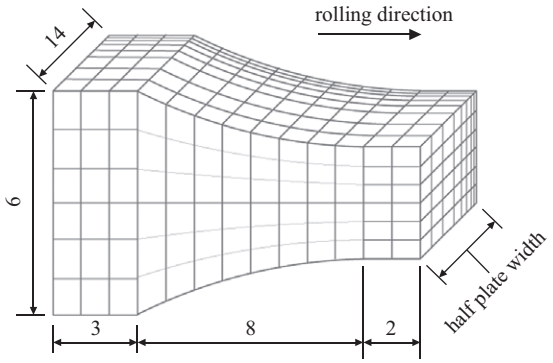


**Fig. 8. The diagram of the FE model.**

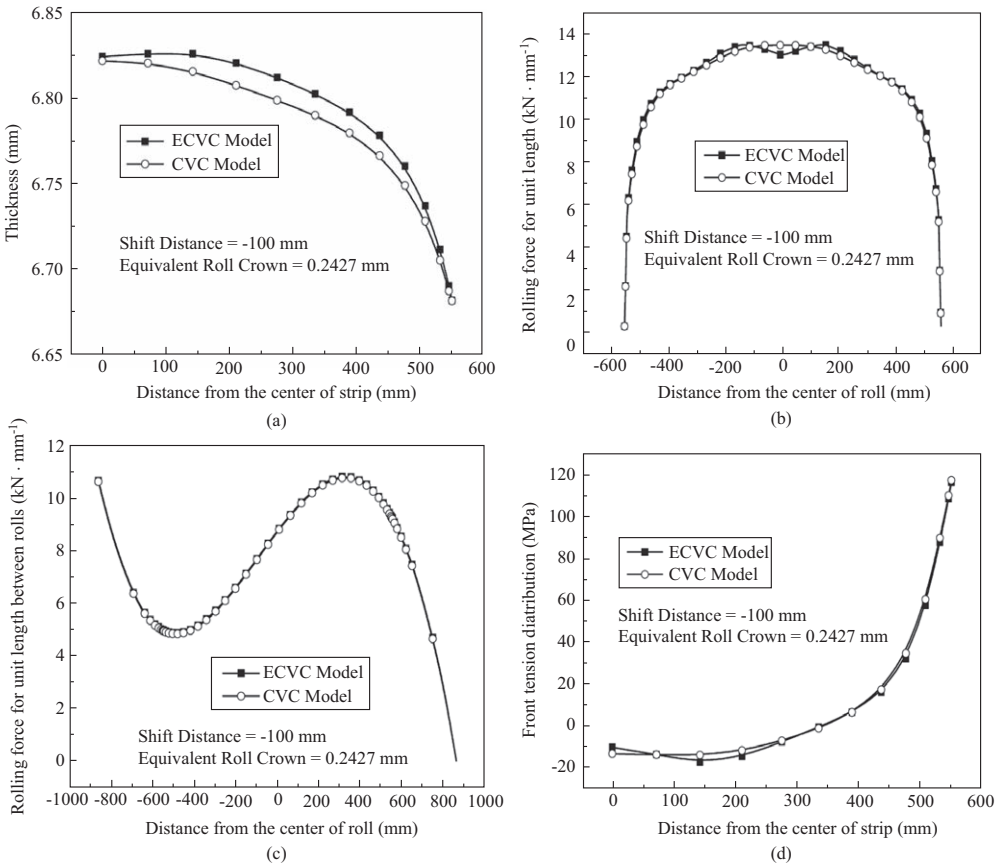


**Fig. 9. Comparison results of ECVC model and CVC model at the axis shifting position 100mm when the equivalent roll crown is 0.2427 mm. (a) Thickness distribution; (b) Rolling force distribution; (c) Rolling force distribution between rolls; (d) Front tension distribution.**

Compared with the traditional model, the equivalent model required two groups of work roll radius parameters; one is used to predict metal deformation by using the RPFEM and the other is used to predict roll deformation by using the unsymmetrical influential function method.

A diagram of the FE model is shown in Fig. 8. The model is

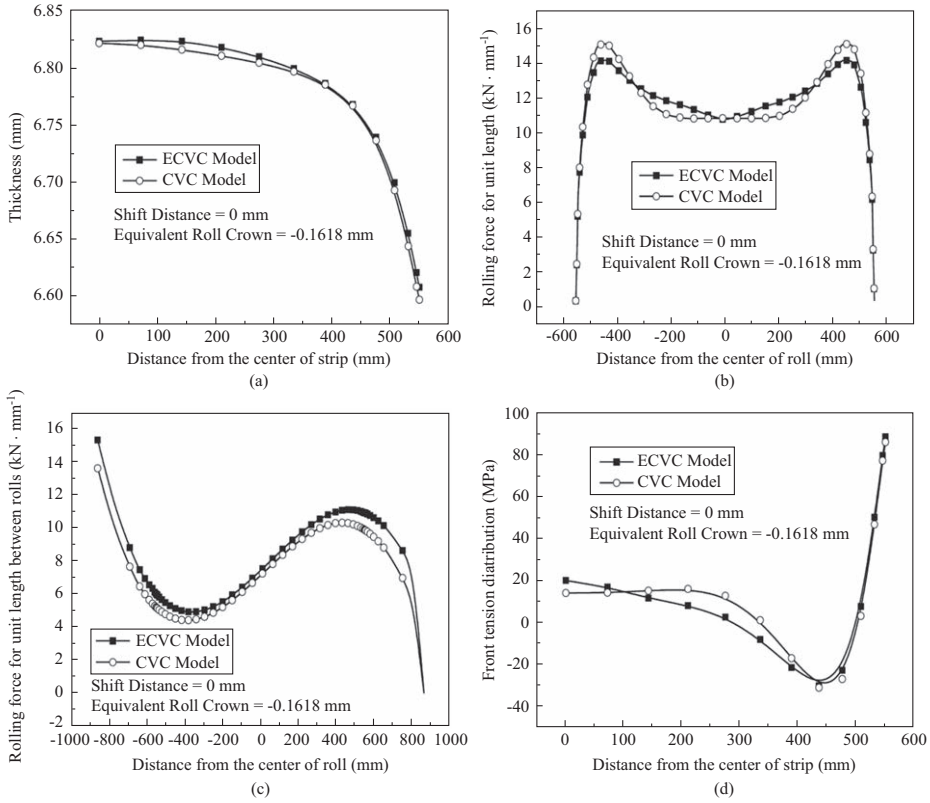


**Fig. 10. Comparison results of ECVC model and CVC model at the axis shifting position 0mm when the equivalent roll crown is 0.1618 mm. (a) Thickness distribution; (b) Rolling force distribution; (c) Rolling force distribution between rolls; (d) Front tension distribution.**

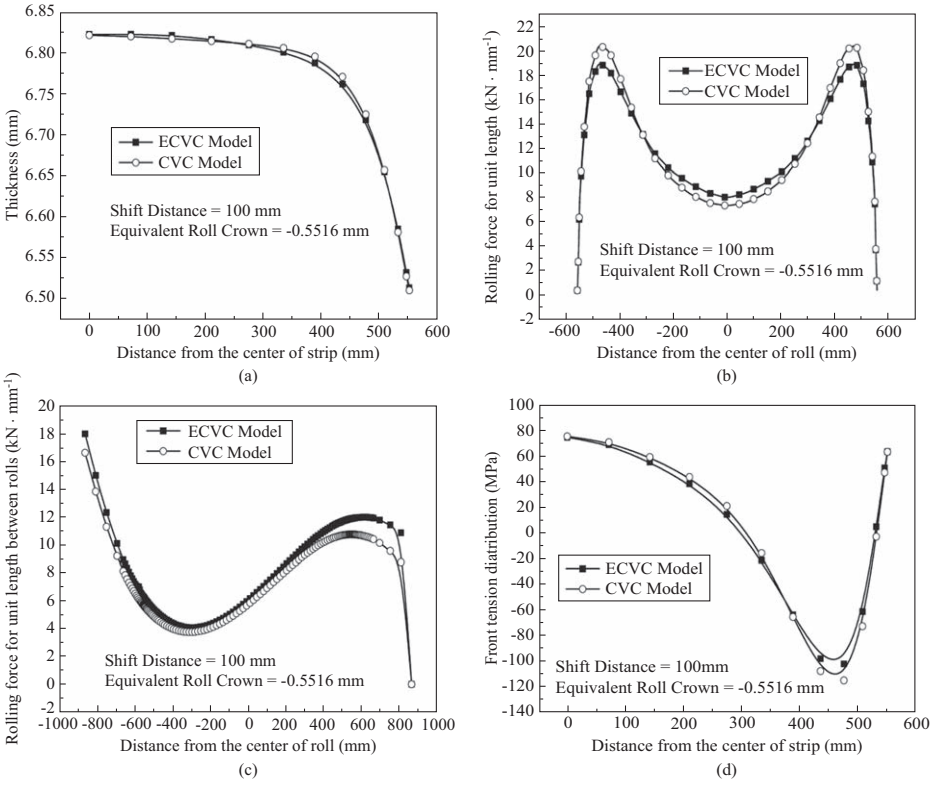


**Fig. 11. Comparison results of ECVC model and CVC model at the axis shifting position 100mm when the equivalent roll crown is 0.5516 mm. (a) Thickness distribution; (b) Rolling force distribution; (c) Rolling force distribution between rolls; (d) Front tension distribution.**

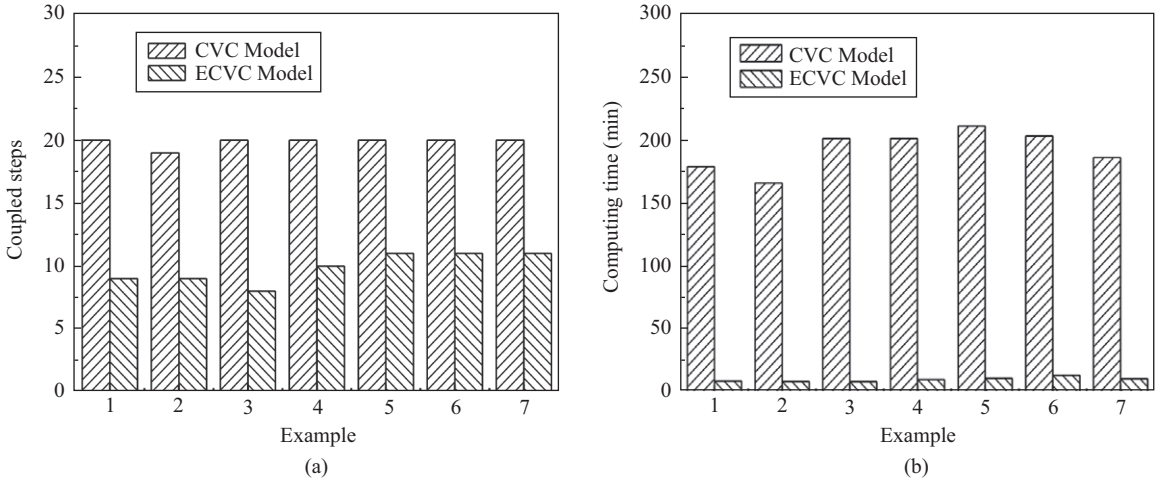


**Fig. 12. Comparison of coupled steps(a) and computing time(b) between CVC model and ECVC model.**

divided into 1092 8-node solid elements, including 14 segments in the width direction (involving the subdivision of the edge by the monotone decrease of a sine function within the range of $[0, \pi/2]$), 6 segments in the thickness direction, 13 segments in the rolling direction, and a grid division diagram. For symmetry, the workpiece is simplified in the quarter model. The friction between the workpiece and the contact surface of the roll follows the Coulomb model of friction. As assumed, the workpiece is incompressible in volume.

## IV. RESULTS AND ANALYSIS

To demonstrate the accuracy of the equivalent model, comparisons of rolling process results of the 4-high CVC mill using the traditional CVC model and ECVC model are illustrated. The parameters used for calculation are shown in Table 4.

The results of comparisons of plate thickness after rolling, rolling force for unit length, and rolling force for unit length between rolls and front tension at different axis shifting distances obtained using the ECVC model and CVC model are shown Figs. 9-11, respectively.

The ECVC model can precisely reflect the influence of shifting the work roll on the control of the strip crown according to the lateral distribution of the exit strip thickness calculated from the positions of the shift rolls, as shown in Figs. 9-11. When the equivalent work roll crown is positive (Fig. 9(a)), the results calculated by the ECVC model differ slightly from those calculated by the CVC model. The maximum deviation located 250 mm from the center point of the strip is approximately 10 μm. When the equivalent work roll crown is negative, the curves of the strip thickness distribution calculated by the two models are in strong agreement (Figs. 10(a) and 11(a)). The maximum deviation value does not exceed 5 μm. The rolling force distributions shown in Figs. 9-11 show that the general trends of the two methods are relatively consistent. The results of the rolling force for unit length, the rolling force for unit length between rolls, and the front tension distribution calculated by the CVC model and ECVC model are highly consistent. Thus, the ECVC model exhibits strong agreement with the traditional CVC model.

Fig. 12 shows the coupled steps, namely the numbers of iterations required for convergence and the computation times of the CVC model and ECVC model under various rolling conditions of a normal 4-high CVC mill. These examples were calculated on a personal computer with Intel Core 2 Dou CPU, a 2-GB memory card, and Windows XP. The number of coupled steps calculated by the ECVC model was only approximately half of the corresponding number calculated by the CVC model, as shown in Fig. 12. The traditional model requires approximately 3 hours to achieve convergence, whereas the ECVC model requires only approximately 10 minutes because of the different meshing methods of the workpieces and rolls. Thus, the ECVC model could decrease computation time by up to 80%.

## V. INDUSTRIAL EXPERIMENT AND VERIFICATION

To verify the accuracy of the ECVC model, the technological parameters and measured plate crown values of the first steel coil-one of the ten rolling schemes shown in Table 5—were extracted from the Baosteel 2050 hot continuous rolling line (CVC rolling mill). The error caused by thermal crown and roll wear can be prevented because the work rolls of the first steel coil in every rolling scheme are new, and thus the calculation result is more reliable. An outlet plate crown comparison between the calculated value and measured value is provided in Table 5 and Fig. 13.

Table 5 shows that the calculated value is close to the measured value. In the ten steel coils, only the calculation error of No. 2 was greater than 10 μm, possibly because of the measurement error. In addition, Fig. 13 shows that the changing laws of the values are identical. Therefore, the ECVC model can accurately reflect the various influences of processing conditions for the plate crown, and thus this model is of high significance in practice.

**Table 5. Outlet plate crown comparison between the calculation value and the measured value.**

| No. | Width (mm) | Outlet thickness (mm) | Outlet plate crown (μm) | | Error (μm) |
|---|---|---|---|---|---|
| | | | Calculated | Measured | |
| 1 | 1267 | 4.66 | 32.5 | 35 | 2.5 |
| 2 | 1108 | 5.13 | 34.0 | 51 | 17.0 |
| 3 | 1248 | 4.62 | 38.0 | 29 | 9.0 |
| 4 | 1313 | 4.67 | 50.2 | 43 | 7.2 |
| 5 | 1236 | 4.07 | 58.6 | 53 | 5.6 |
| 6 | 1192 | 5.64 | 18.3 | 23 | 4.7 |
| 7 | 1267 | 5.85 | 36.2 | 33 | 3.2 |
| 8 | 1262 | 4.13 | 69.3 | 64 | 5.3 |
| 9 | 1230 | 5.65 | 47.5 | 38 | 9.5 |
| 10 | 1112 | 5.65 | 28.4 | 35 | 6.6 |

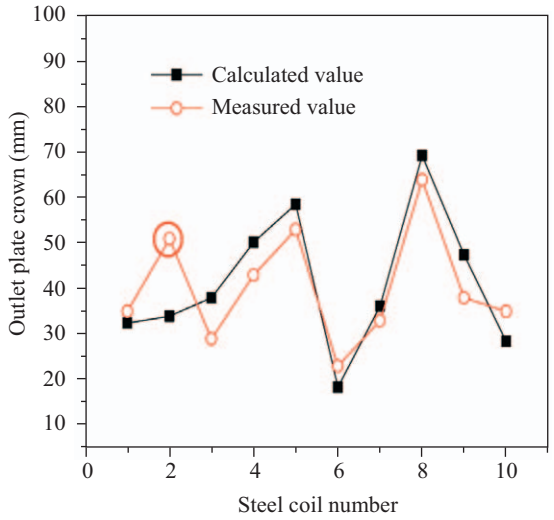


**Fig. 13. Comparison of the change trend between calculated value and measured value of outlet plate crown.**

## VI. CONCLUSIONS

1. A coupling simulation system based on a 3D RPFEM, elastic-plastic FEM, and influential function method was developed.
2. A reasonable combination algorithm is proposed to deal with the interaction between the quarter model for the analysis of metal plastic deformation and the half model for the analysis of the elastic deformation of rolls, in order to achieve the dual objective of high precision and high efficiency.
3. The distribution of rolling force can reasonable be regarded as symmetrical according to the force equilibrium of the work-piece. The numerical results revealed that the ECVC model can reduce the number of iterations by approximately 50% and the computation time by approximately 80%. Finally, the accuracy of the ECVC model was verified by the calculated value and measured plate crown values from the Baosteel 2050 hot continuous rolling line.

## ACKNOWLEDGEMENTS

This project are supported by Major program of national natural science foundation of China (Grant No. U1710254), National natural science foundation of China (Grant No. 51804215), Shanxi Province science and technology major project (Grant No. MC2016-01), Shanxi province science and technology major projects (Grant No. 20181102015), Natural science foundation of Shanxi Province (Grant No. 201701D221143), Taiyuan city science and technology major projects (Grant No. 170203), key research and development program of Shanxi Province (Grant No. 201703D111003).

## REFERENCES

Chen, Z. J. and H. Xiao (2012). The fast multipole boundary element methods (fmbem) and its applications in rolling engineering analysis. Computational Mechanics 50(5), 513-531.

Du, F. S., M. T. Wang and X. T. Li (2007). Research on deformation and micro-structure evolution during forging of large-scale parts. Journal of Materials Processing Technology 187-188, 591-594.

Daun, J., Y. Kang, Y. J. Jang, D. Lee and S. Won (2013). Development of FEM simulator combined with camber reducing output; Feedback fuzzy controller for rough rolling process. ISIJ international 53(3), 511-519.

Hwang, S. M., C. G. Sun, S. R. Ryoo and W. J. Kwak (2002). An integrated FE process model for precision analysis of thermo-mechanical behaviors of rolls and strip in hot strip rolling. Computer Methods in Applied Mechanics and Engineering 191(37-38), 4015-4033.

Kawanamt, T. and H. Matsumoto (1983). Development of various methods of shape and crown control in strip rolling. Tetsu-to-Hagane 69(3), 348-356.

Kainz, A. J., M. E. Widder and K. Zeman (2013). Enhanced strip-roll coupling concepts for the numerical simulation of flat hot rolling. Acta Mechanica 224(5), 957-983.

Kim, S. H., J. H. Lee, W. J. Kwak and S. M. Hwang (2005). Dimensional analysis of hot strip rolling for on-line prediction of Thermo-mechanical behavior of roll-strip system. ISIJ International 45(2), 199-208.

Kim, T. H., W. H. Lee and S. M. Hwang (2003). An integrated FE process model for the prediction of strip profile in flat rolling. ISIJ international 43(12), 1947-1956.

Liu, H. M., Z. Z. Zheng and Y. Peng (2001). Streamline strip element method for analysis of the three-dimensional stresses and deformations of strip rolling. International Journal for Numerical Methods in Engineering 50(5), 1059-1076.

Liu, H. M., D. Jin and Y. R. Wang (2004). Strip layer method for simulation of the three-dimensional deformations of plate and strip rolling. Communications in Numerical Methods in Engineering 20(3), 183-191.

Lee, J. S., T. J. Shin, S. J. Yoon and S. M. Hwang (2016). Prediction of Steady-State Strip Profile in Flat Rolling. Steel Research International 87(7), 930-940.

Linghu, K., Z. Y. Jiang, J. W. Zhao, F. Li, D. B. Wei, J. Z. Xu and X. M, Zhao (2014). 3D FEM analysis of strip shape during multi-pass rolling in a 6-high CVC cold rolling mill. The International Journal of Advanced Manufacturing Technology 74, 1733-1745.

Liu, C., P. Hartley, C. E. N. Sturgess and G. W. Rowe (1985). Elastic-plastic finite-element modelling of cold rolling of strip. International Journal of Mechanical Sciences 27(7-8), 531-541.

Nakhoul, R., P. Montmitonnet and N. Legrand (2014). Manifested flatness defect prediction in cold rolling of thin strips. International Journal of Material Forming 8(2), 283-292.

Schmidtchen, M. and R. Kawalla (2016). Fast numerical simulation of symmetric flat rolling processes for inhomogeneous materials using a layer model-part i: basic theory. Steel Research International 87(8), 1065-1081.

Takaaki, I. and I. Yarita (1991). 3-dimensional Analysis of flat rolling by rigid-plastic FEM considering sticking and slipping frictional boundary. ISIJ International 31(6), 559-565.

Wang, T., H. Xiao, T. Y. Zhao and X. D. Qi (2012). Improvement of 3-D FEM coupled model on strip crown in hot rolling. Journal of Iron and Steel Research International 19(3), 14-19.

Wang, K. and Z. Chen (2015). An efficient FEM-BEM coupling method in wave radiation problem analysis of oil platforms with complicated geometry. Engineering Analysis with Boundary Elements 58, 18-25.

Wang, X. D., F. Li, B. Li, L. Dong and B. Zhang (2012). Design and application of an optimum backup roll contour configured with CVC work roll in hot strip mill. ISIJ international 52(9), 1637-1643.

Wang, M., X. T. Li, F. S. Du and Y. Z. Zheng (2005). A coupled thermal-mechanical and microstructural simulation of the cross wedge rolling process and experimental verification. Materials Science and Engineering: A 391(1-2), 305-312.

Wang, Y. R., Z. S. Cui and J. G. Yuan (2005). Simulation of rolling process on 4-high CVC hot strip continuous mills. IRON AND STEEL 12, 46-49.

Wood, G. E., K. Humphries and P. W. Arnold (1989). Modernization of a Hot Strip Mill With CVC Technology and a New Roughing Mill With Automatic Width Control. Metall Plant Technol Int 5, 92-109.

Yanagimoto, J. (2002). Strategic FEM simulator for innovation of rolling mill and process. Journal of Materials Processing Technology 130, 224-228.

Zhang, Q., X. Sun and J. Bai (2007). Analysis of roll's elastic deformation on CVC 6-hi mill by FEM, China Mechanical Engineering 7, 789-792.